DISCUSSION

The present study demonstrated the presence of anti-Tom40 antibodies more frequently in the serum of patients with AD than control subjects or patients with multiple sclerosis (Table 1). We do not find any differences in anti-Tom40 antibodies between control subjects without neurological diseases older than 60 years and healthy control subjects younger than 40 years. This indicates that it may not be age dependent. The finding of anti-Tom40 antibodies in patients with AD suggests that the anti-Tom40 antibody may be a potential biomarker of AD. Further prospective studies are required to establish the anti-Tom40 antibody as biomarker of AD.

The brain in AD is characterized by impairments in energy metabolism and vascular hypoperfusion [10]. Mitochondrial abnormalities and vascular damage are important in the pathogenesis of AD, but causative factors in mitochondrial dysfunction in AD are not well understood [11–13]. The translocase of the outer membrane (TOM) complex is a protein complex of the outer mitochondrial membrane essential for protein transport into mitochondria, and Tom40, a channel-forming subunit of the TOM complex, has been associated with AD [8, 14–20]. A variable length, deoxythymidine homopolymer (poly-T) within intron 6 of the Tom40 gene is associated with the age of onset of late-onset AD [8]. Furthermore, nonglycosylated full length and C-terminal truncated amyloid-β protein precursor (AβPP) accumulates in the protein import channels of mitochondria of brains of patients with AD but not in age-matched controls [17]. AβPP forms a stable complex (480 kDa) with Tom40 and a larger complex (620 kDa) with both Tom40 and the translocase of the inner membrane (TIM) complex Tim23, and accumulation of AβPP across mitochondrial import channels may lead to mitochondrial dysfunction [17, 18]. It has been also shown that the transport of amyloid-β into the mitochondrion is mediated by the Tom40 pore, further promoting neurotoxity [19, 20]. The present study showed an association between anti-Tom40 antibody and lower cognitive scores in patients with AD (Table 2). This result provided evidence in support of the previously reported hypothesis that Tom40 may be important in the pathogenesis of cognitive impairment in AD.

The mechanism of anti-Tom40 antibody production is unclear. AβPP may form complexes with Tom40 and may cause mitochondrial dysfunction and endothelial and neuronal cell damage. An immune response after formation of these complexes may induce the production of the anti-Tom40 antibody. An additional mechanism of anti-Tom40 antibody production might be considered. The aberrant Tom40 may lead to formation of antibodies against Tom40 and may lead to mitochondrial dysfunction. These possible mechanisms may cause inadequate availability of energy in the form of adenosine triphosphate (ATP) in the endothelial cell, potentially resulting in vascular dysfunction. It also may lead to inadequate availability of ATP in active dendrites and axons resulting in an impediment of axodendritic flow to synapses, resulting in losses of synapses and cognitive impairment.

The pathogenetic role of anti-Tom40 antibody in AD is unknown. The antigen Tom40 is an intracellular protein, not on the surface of the cell membrane. Based on the intracellular location of the antigen, the anti-Tom40 antibody may not be related to pathogenicity. However, some reports indicate that the selective autoantibody penetrates living cell membranes and binds to intracellular antigens [21, 22]. Similarly, anti-Tom40 antibody may penetrate cell membranes and bind to Tom40; this may potentially inhibit the function of Tom40, which is essential for protein transport into mitochondria, and may cause mitochondrial dysfunction and contribute to the pathogenesis of AD. Future study may include an evaluation of whether anti-Tom40 antibody could penetrate cell membranes and bind to Tom40, resulting in mitochondrial dysfunction.

The limitations of the present study include the small number of patients and control subjects. Future studies may include larger numbers of subjects to establish a relationship between anti-Tom40 antibody and cognitive impairment in patients with AD.

ACKNOWLEDGMENTS

This study was supported, in part, by a Japanese Health and Labor Sciences Research Grant for Comprehensive Research on Disability Health and Welfare (09158512).

Authors' disclosures available online (http://www.j-alz.com/disclosures/view.php?id=1089).

REFERENCES

[1] Grammas P, Yamada M, Zlokovic B (2002) The cerebromicrovasculature: A key player in the pathogenesis of Alzheimer's disease. *J Alzheimers Dis* **4**, 217-223.

[2] Zlokovic BV (2002) Vascular disorder in Alzheimer's disease: Role in pathogenesis of dementia and therapeutic targets. *Adv Drug Deliv Rev* **54**, 1553-1559.

[3] Grammas P, Samany PG, Thirumangalakudi L (2006) Thrombin and inflammatory proteins are elevated in Alzheimer's

disease microvessels: Implications for disease pathogenesis. *J Alzheimers Dis* **9**, 51-58.

[4] Christov A, Ottman JT, Grammas P (2004) Vascular inflammatory, oxidative and protease-based processes: Implications for neuronal cell death in Alzheimer's disease. *Neurol Res* **26**, 540-546.

[5] Loeffler DA, Juneau PL, Nguyen HU, Najman D, Pomara N, LeWitt PA (1997) Immunocytochemical detection of antihippocampal antibodies in Alzheimer's disease and normal cerebrospinal fluid. *Neurochem Res* **22**, 209-214.

[6] Bouras C, Riederer BM, Kövari E, Hof PR, Giannakopoulos P (2005) Humoral immunity in brain aging and Alzheimer's disease. *Brain Res Brain Res Rev* **48**, 477-487.

[7] Vacirca D, Barbati C, Scazzocchio B, Masella R, Rosano G, Malorni W, Ortona E (2011) Anti-ATP synthase autoantibodies from patients with Alzheimer's disease reduce extracellular HDL level. *J Alzheimers Dis* **25**, 1-5.

[8] Roses AD, Lutz MW, Amrine-Madsen H, Saunders AM, Crenshaw DG, Sundseth SS, Huentelman MJ, Welsh-Bohmer KA, Reiman EM (2010) A TOMM40 variable-length polymorphism predicts the age of late-onset Alzheimer's disease. *Pharmacogenomics J* **10**, 375-384.

[9] Toda T, Kimura N (1997) Standardization of protocol for Immobiline 2-D PAGE and construction of 2-D PAGE protein database on World Wide Web home page. *Jpn J Electrophoresis* **41**, 13-19.

[10] Murray IV, Proza JF, Sohrabji F, Lawler JM (2011) Vascular and metabolic dysfunction in Alzheimer's disease: A review. *Exp Biol Med* **236**, 772-782.

[11] Aliev G, Seyidova D, Lamb BT, Obrenovich ME, Siedlak SL, Vinters HV, Friedland RP, LaManna JC, Smith MA, Perry G (2003) Mitochondria and vascular lesions as a central target for the development of Alzheimer's disease and Alzheimer disease-like pathology in transgenic mice. *Neurol Res* **25**, 665-674.

[12] Gibson GE, Shi Q (2010) A mitocentric view of Alzheimer's disease suggests multi-faceted treatments. *J Alzheimers Dis* **20**(Suppl 2), S591-S607.

[13] Santos RX, Correia SC, Wang X, Perry G, Smith MA, Moreira PI, Zhu X (2010) A synergistic dysfunction of mitochondrial fission/fusion dynamics and mitophagy in Alzheimer's disease. *J Alzheimers Dis* **20**(Suppl 2), S401-S412.

[14] Humphries AD, Streimann IC, Stojanovski D, Johnston AJ, Yano M, Hoogenraad NJ, Ryan MT (2005) Dissection of the mitochondrial import and assembly pathway for human Tom40. *J Biol Chem* **280**, 11535-11543.

[15] Hong MG, Alexeyenko A, Lambert JC, Amouyel P, Prince JA (2010) Genome-wide pathway analysis implicates intracellular transmembrane protein transport in Alzheimer disease. *J Hum Genet* **55**, 707-709.

[16] Roses AD (2010) An inherited variable poly-T repeat genotype in TOMM40 in Alzheimer disease. *Arch Neurol* **67**, 536-541.

[17] Devi L, Prabhu BM, Galati DF, Avadhani NG, Anandatheerthavarada HK (2006) Accumulation of amyloid precursor protein in the mitochondrial import channels of human Alzheimer's disease brain is associated with mitochondrial dysfunction. *J Neurosci* **26**, 9057-9068.

[18] Anandatheerthavarada HK, Biswas G, Robin MA, Avadhani NG (2003) Mitochondrial targeting and a novel transmembrane arrest of Alzheimer's amyloid precursor protein impairs mitochondrial function in neuronal cells. *J Cell Biol* **161**, 41-54.

[19] Hansson Petersen CA, Alikhani N, Behbahani H, Wiehager B, Pavlov PF, Alafuzoff I, Leinonen V, Ito A, Winblad B, Glaser E, Ankarcrona M (2008) The amyloid beta-peptide is imported into mitochondria via the TOM import machinery and localized to mitochondrial cristae. *Proc Natl Acad Sci U S A* **105**, 13145-13150.

[20] Grossman I, Lutz MW, Crenshaw DG, Saunders AM, Burns DK, Roses AD (2010) Alzheimer's disease: Diagnostics, prognostics and the road to prevention. *EPMA J* **1**, 293-303.

[21] Deng SX, Hanson E, Sanz I (2000) *In vivo* cell penetration and intracellular transport of anti-Sm and anti-La autoantibodies. *Int Immunol* **12**, 415-123.

[22] Seddiki N, Nato F, Lafaye P, Amoura Z, Piette JC, Mazié JC (2001) Calreticulin, a potential cell surface receptor involved in cell penetration of anti-DNA antibodies. *J Immunol* **166**, 6423-6429.

INTERNAL MEDICINE

□ ORIGINAL ARTICLE □

Late-onset Patients with Sporadic Amyotrophic Lateral Sclerosis in Japan have a Higher Progression Rate of ALSFRS-R at the Time of Diagnosis

Yuji Tanaka, Nobuaki Yoshikura, Naoko Harada, Megumi Yamada, Akihiro Koumura, Takeo Sakurai, Yuichi Hayashi, Akio Kimura, Isao Hozumi and Takashi Inuzuka

Abstract

Objective The population in Japan is aging at a faster rate than in other countries in the world. It is speculated that the number of patients with late-onset amyotrophic lateral sclerosis (ALS) will increase even more in the future. However, few studies have been undertaken on the characteristics of patients with late-onset ALS in Japan. This study sought to investigate the clinical features of patients with late-onset ALS compared with those with early-onset ALS using the progression rate (ΔFS).

Methods Forty-five patients with sporadic ALS were divided into 2 groups: 23 patients with early-onset of ALS (<65 years; early onset) and 22 patients with late-onset ALS (≥65 years; late onset). Every patient was followed up from the time of initial diagnosis to the primary endpoint (death or time culminating in death without tracheostomy or ventilation assistance including noninvasive positive pressure ventilation) or for at least 48 months after initial diagnosis.

Results ΔFS in the patient group with late onset was significantly higher than that of the group with early onset (p=0.010). Survival of patients with late onset was significantly decreased compared to that of patients with early onset (p=0.031).

Conclusion Our finding suggested that patients with late-onset ALS showed more rapid disease progression than those with early-onset ALS using ΔFS.

Key words: amyotrophic lateral sclerosis, late onset, progression rate, rapidly progression

(Intern Med 51: 579-584, 2012)
(DOI: 10.2169/internalmedicine.51.6148)

Introduction

Amyotrophic lateral sclerosis (ALS) is the most common and best recognized form of motor neuron diseases. ALS is a degeneration of both upper and lower motor neurons leading to progressive muscular paralysis with death usually within 1 to 5 years after the onset (1).

The incidence rate of ALS varies with the age at onset. Some studies have reported that the age at onset of ALS is higher now compared to 2 or 3 decades ago (2-6). Previous reports described that late onset of ALS was a risk factor for poor prognosis (7-10).

The population in Japan is aging at a faster rate than in other countries in the world (11). It is speculated that the number of patients with late-onset ALS will increase even more in the future. However, few studies have been undertaken on the characteristics of patients with late-onset ALS in Japan. It is important to study the characteristics of this disease because the aging population is increasing worldwide.

Recently, the progression rate (ΔFS) of the revised ALS functional rating scale (ALSFRS-R) (12) at the time of diagnosis was reported to be useful for the quantitative assessment of patients with ALS (13). Subsequently, to our knowledge, this is the first report of clinical features associated with ΔFS. Herein, we describe the clinical features of patients with late-onset ALS and compare them with those of

Department of Neurology and Geriatrics, Graduate School of Medicine, Gifu University, Japan
Received for publication July 11, 2011; Accepted for publication December 4, 2011
Correspondence to Dr. Yuji Tanaka, yutanaka-gif@umin.net

Table 1. Summary of Clinical Characteristics between Early- and Late-onset Amyotrophic Lateral Sclerosis Patient Groups

	Early-onset ALS patients group (n=23)	Late-onset ALS patients group (n=22)	p value
Age (years)	59.0 (30-64)	76.5 (66-89)	p<0.001
Sex (M/F)	16/7	15/7	p>0.999
Onset Bulbar onset	6	11	0.215
Limb onset	16	11	
ALSFRS-R	41.0 (2-48)	35.5 (5-46)	0.075
Duration (m)	17.0 (3-68)	12.5 (3-134)	0.225
Progression rate	0.57 (0.04-2.71)	1.01 (0.15-4.00)	0.010

Variables are expressed as median (range). Medians were compared using the Mann-Whitney *U* test. Categorical variables were compared using Fisher exact probability test. ALSFRS-R: revised Amyotrophic lateral sclerosis Functional Rating Scale at initial diagnosis. Duration: from the time when the initial symptoms were noted to diagnosis (months), progression rate (ΔFS); 48-ALSFRS-R at time of diagnosis/duration from the time when the initial symptoms were noted to diagnosis (months).

patients with early-onset ALS using ΔFS.

Materials and Methods

Patients

The present study population consisted of 45 patients with sporadic ALS. On the basis of the El Escorial/Airlie House criteria (14), the diagnosis of clinically definite or clinically probable ALS was made between 1999 and 2005. All ALS patients were consecutively consulted at our hospital and interviewed by neurologists. Every patient underwent serum and cerebrospinal fluid examination, cranial and spinal cord magnetic resonance imaging, evoked motor and sensory potential examinations, electromyogram, and functional respiratory tests. Patients with clinically probable ALS were later confirmed as having definite ALS. The onset of illness was the time of progressive weakness in any body part ascertained by multiple family and patient interviews and consultation with the first visited physicians. Each patient was followed up from the time of initial diagnosis to the primary endpoint (death or time culminating in death without tracheostomy or ventilatory assistance including noninvasive positive pressure ventilation) or for at least 48 months after initial diagnosis.

Patients were divided into 2 groups: 23 patients with early-onset ALS (<65 years; early onset; 16 men, 7 women; median age, 55.3 years; range, 30-64 years) and 22 patients with late-onset ALS (≥65 years; late onset; 15 men, 7 women; median age, 75.6 years; range, 66-89 years). The 2 groups were compared for initial symptoms, ALSFRS-R score at the time of initial diagnosis, duration (from the time when the initial symptoms were noted to diagnosis) and ΔFS (13). ΔFS was calculated as ΔFS=(48-ALSFRS-R score at time of diagnosis)/duration from the time when the initial symptoms were noted to diagnosis (months) (13). The time of initial onset was determined on the basis of subjective complaints and information confirmed from family members. Data for ΔFS represented a fixed covariate at the baseline of diagnosis (13).

Statistical analysis

Categorical variables were compared using the Fisher exact probability test. Other variables are expressed as median (range). Medians were compared using the Mann-Whitney *U* test. The association between age categories and post-diagnosis period until primary endpoint were examined using the Kaplan-Meier curve, and differences were analyzed using the log-rank test and Cox proportional hazards model. All analyses were carried out using StatView statistical software, version 5.0 (Abacus Concepts, Inc., Berkeley, CA). Values for p less than 0.05 were considered significant.

Results

The clinical features of the patients with ALS are summarized in Table 1. In the ALS patient group with early onset, 6 patients were bulbar onset and 16 patients were limb onset. In those with late onset, 11 patients were bulbar onset and 10 patients were limb onset. There was no significant difference between ALS patients with bulbar onset and limb onset in each group (p=0.215). The ALSFRS-R score at the time of initial diagnosis was not significantly different in patients with early onset (median, 41.0 points; range; 2-48

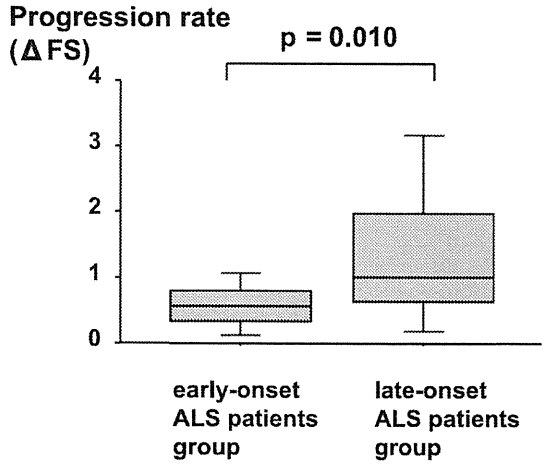

Figure 1. Comparison between the progression rate of the early- and late-onset amyotrophic lateral sclerosis patients groups. The progression rate (ΔFS) was different in the patient group with early-onset amyotrophic lateral sclerosis (ALS) (median, 0.57; range 0.04-2.71) compared with the group with late-onset ALS (median, 1.01; range, 0.15-4.00). ΔFS of the late-onset ALS group was significantly higher than that of the early-onset ALS group (p=0.010).

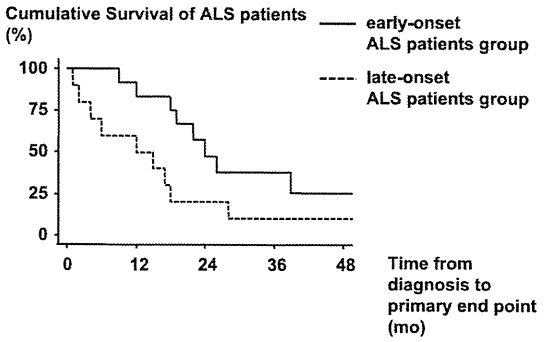

Figure 2. Kaplan-Meier survival plots according to age at onset and post-diagnosis period until primary endpoint in amyotrophic lateral sclerosis patients. Kaplan-Meier survival plots according to the age at onset and post-diagnosis period until primary endpoint (death or time culminating in death without tracheostomy or ventilation assistance) in amyotrophic lateral sclerosis patients (n=45) are shown. By using simple, nominal variables in the Cox proportional hazards model, the survival of patients with late onset (n=22) was significantly decreased compared to that of patients with early onset (n=23; p=0.031).

points) compared with those with late onset (median, 35.5 point; range, 5-46 points; p=0.075). The duration was not significantly different in patients with early onset (median, 17.0 months; range, 3-68 months) compared with those with late onset (median, 12.5 months; range, 3-134 months; p= 0.225). ΔFS was significantly different in patients with early onset (median, 0.57; range, 0.04-2.71) compared with those with late onset (median, 1.01; range, 0.15-4.00; p=0.010) (Fig. 1). Using simple, nominal variables in the Cox proportional hazards model, survival was found to differ between patients with early onset and those with late onset. Survival of patients with late onset was significantly decreased compared with patients with early onset (p=0.031) (Fig. 2).

The clinical features of the ALS patients with bulbar onset are summarized in Table 2. The ALSFRS-R score at the time of initial diagnosis was not significantly different in early onset patients with bulbar onset (median, 43.5 points; range; 3-46 points) compared with late onset patients with bulbar onset (median, 35.0 point; range, 5-46 points; p= 0.057). The duration was not significantly different in early onset patients with bulbar onset (median, 10.5 months; range, 3-28 months) compared with late onset patients with bulbar onset (median, 11.0 months; range, 3-27 months; p= 0.880). ΔFS was significantly different in early onset patients with bulbar onset (median, 0.47; range, 0.14-1.75) compared with late onset patients with bulbar onset (median, 2.00; range, 0.15-4.00; p=0.044) (Fig. 3). Using simple, nominal variables in the Cox proportional hazards model, survival was found to differ between early onset patients and late onset patients with bulbar onset. Survival of patients with late onset was significantly decreased compared with patients with early onset (p=0.031) (Fig. 4).

The clinical features of the ALS patients with limb onset are summarized in Table 3. The ALSFRS-R score at the time of initial diagnosis was not significantly different in early onset patients with limb onset (median, 39.5 points; range; 4-48 points) compared with late onset patients with limb onset (median, 36.0 point; range, 14-45 points; p= 0.349). The duration was not significantly different in early onset patients with limb onset (median, 21.0 months; range, 3-68 months) compared with late onset patients with limb onset (median, 13.0 months; range, 7-134 months; p=0.505). ΔFS was significantly different in early onset patients with limb onset (median, 0.54; range, 0.04-0.91) compared with late onset patients with limb onset (median, 0.76; range, 0.18-1.71; p=0.046) (Fig. 5). Using simple, nominal variables in the Cox proportional hazards model, survival was found to differ between early onset patients and late onset patients with bulbar onset. Survival of patients with late onset was significantly decreased compared with patients with early onset (p=0.034) (Fig. 6).

Discussion

In this study, we demonstrated that ΔFS of the late-onset ALS group was significantly higher than that of the early-onset ALS group. Moreover, even in both groups with bulbar and limb onset, we demonstrated that ΔFS of the late-onset ALS group was significantly higher than that of the early-onset ALS group. These results showed that ALS in the group with late onset was rapidly progressing. In addition, the survival of patients with late onset was significantly decreased compared with that of patients of early onset.

Recently, ΔFS of ALS was reported and calculated on the

Table 2. Summary of Clinical Characteristics between Early- and Late-onset Amyotrophic Lateral Sclerosis Patient Groups with Bulbar Onset

	Early-onset ALS patients group (n=6)	Late-onset ALS patients group (n=11)	p value
Age (years)	52.5 (30-64)	77.0 (66-89)	p<0.001
Sex (M/F)	4/2	7/4	p>0.999
ALSFRS-R	43.5 (39-46)	35.0 (5-46)	0.057
Duration (m)	10.5 (3-28)	11.0 (3-27)	0.880
Progression rate	0.47 (0.14-1.75)	2.00 (0.15-4.00)	0.044

Variables are expressed as median (range). Medians were compared using the Mann-Whitney *U* test. Categorical variables were compared using Fisher exact probability test. ALSFRS-R: revised Amyotrophic lateral sclerosis Functional Rating Scale at initial diagnosis. Duration: from the time when the initial symptoms were noted to diagnosis (months), progression rate (ΔFS); 48-ALSFRS-R at time of diagnosis/duration from the time when the initial symptoms were noted to diagnosis (months).

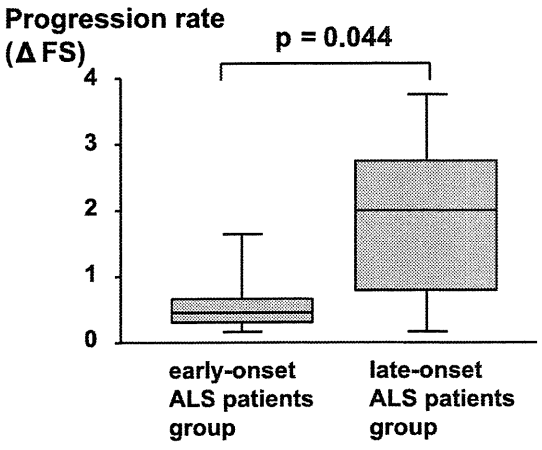

Figure 3. Comparison between the progression rate of early- and late-onset amyotrophic lateral sclerosis patients groups with bulbar onset. The progression rate (ΔFS) was different in the patient group with early-onset amyotrophic lateral sclerosis (ALS) (median, 0.47; range 0.14-1.75) compared with the group with late-onset ALS (median, 2.00; range, 0.15-4.00). ΔFS of the late-onset ALS group was significantly higher than that of the early-onset ALS group (p=0.044).

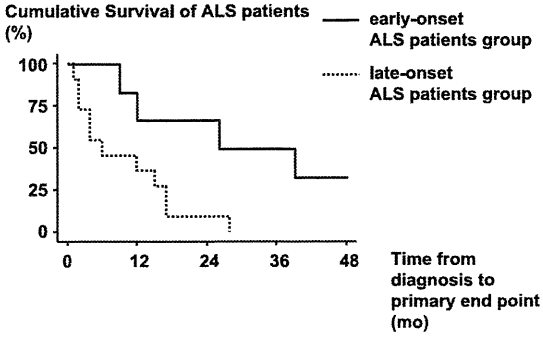

Figure 4. Kaplan-Meier survival plots according to the age at onset and of post-diagnosis period until primary endpoint in amyotrophic lateral sclerosis patients with bulbar onset. Kaplan-Meier survival plots according to the age at onset and post-diagnosis period until primary endpoint (death or time culminating in death without tracheostomy or ventilation assistance) in amyotrophic lateral sclerosis patients (n=17) are shown. By using simple, nominal variables in the Cox proportional hazards model, the survival of patients with late onset (n=11) was significantly decreased compared to that of patients with early onset (n=6; p=0.031).

basis of the severity (ALSFRS-R) and duration (from the time when the initial symptoms were noted to diagnosis) (13). ΔFS calculated by using the ALSFRS-R score at the time of initial diagnosis and symptom duration represents a predictive index of survival. It enables evaluation of the disease process. In addition, ΔFS at the time of diagnosis in each patient appears to be more closely associated with future progression to the primary endpoint (13). It was reported the significance of ΔFS by adding a time axis at diagnosis and conducting comparisons with the total ALSFRS-R score alone (13). Subsequently, to our knowledge, this is the first report of an association between clinical features and ΔFS.

In the present study, ALSFRS-R score and duration (from the time when the initial symptoms were noted to diagnosis) were not significantly different between ALS patients with early onset and those with late onset. However, ΔFS of late-onset ALS group was significantly higher than that of the early-onset ALS group. Survival of patients with late onset was significantly decreased compared with that of patients with early onset. It was suggested that ΔFS might predict the prognosis more accurately (13).

Table 3. Summary of Clinical Characteristics between Early- and Late-onset Amyotrophic Lateral Sclerosis Patient Groups with Limb Onset

	Early-onset ALS patients group (n=16)	Late-onset ALS patients group (n=11)	p value
Age (years)	59.0 (36-64)	73.0 (66-82)	p<0.001
Sex (M/F)	11/5	8/3	p>0.999
ALSFRS-R	39.5 (4-48)	36.0 (14-45)	0.349
Duration (m)	21.0 (3-68)	13.0 (7-134)	0.505
Progression rate	0.54 (0.04-0.91)	0.76 (0.18-1.71)	0.046

Variables are expressed as median (range). Medians were compared using the Mann-Whitney *U* test. Categorical variables were compared using Fisher exact probability test. ALSFRS-R: revised Amyotrophic lateral sclerosis Functional Rating Scale at initial diagnosis. Duration: from the time when the initial symptoms were noted to diagnosis (months), progression rate (ΔFS); 48-ALSFRS-R at time of diagnosis/duration from the time when the initial symptoms were noted to diagnosis (months).

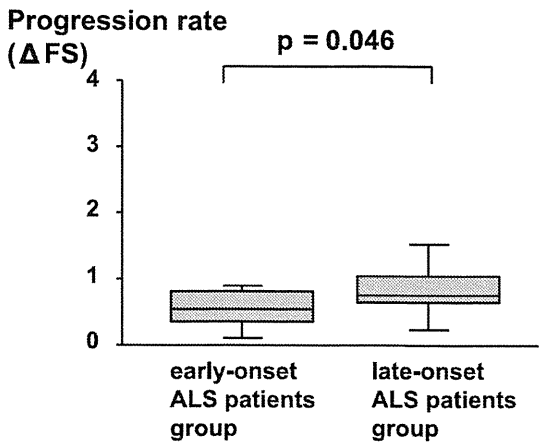

Figure 5. Comparison between the progression rate of early- and late-onset amyotrophic lateral sclerosis patients groups with limb onset. The progression rate (ΔFS) was different in the patient group with early-onset amyotrophic lateral sclerosis (ALS) (median, 0.54; range 0.04-0.91) compared with the group with late-onset ALS (median, 0.76; range, 0.18-1.71). ΔFS of the late-onset ALS group was significantly higher than that of the early-onset ALS group (p=0.046).

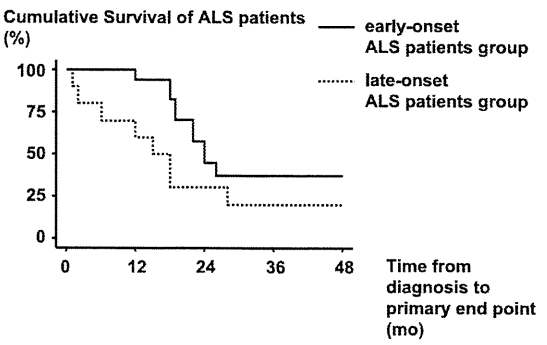

Figure 6. Kaplan-Meier survival plots according to the age at onset and of post-diagnosis period until primary endpoint in amyotrophic lateral sclerosis patients with limb onset. Kaplan-Meier survival plots according to the age at onset and post-diagnosis period until primary endpoint (death or time culminating in death without tracheostomy or ventilation assistance) in amyotrophic lateral sclerosis patients (n=27) are shown. By using simple, nominal variables in the Cox proportional hazards model, the survival of patients with late onset (n=11) was significantly decreased compared to that of patients with early onset (n=16; p=0.034).

A previous study had reported that patients with late-onset ALS had a poor prognosis (15). In this regard, it was speculated that the degeneration of motor neurons was relevant in the aging process (15). However, degeneration of motor neurons in ALS was reported to be different from that in the normal aging process. In addition, it was surmised that a poor prognosis was affected by age-related physiological respiratory insufficiency rather than by age-related of motor neurons (16). The age at onset of ALS is higher now compared to the recent 2 or 3 decades (2-6). This might be related to the longer life expectancy of the general population. Although the increase in mortality is restricted to the population aged ≥65 years, it cannot be explained by the increasing age of the general population alone (17). It was formerly reported that elderly people with ALS were less likely to consult a neurologic specialist (18). Recently, it was thought that elderly people consult neurologists more often (19). Thus, it was thought that the clinical features of patients with late-onset ALS were related to pathological, physiological and medical-sociological factors.

The population in Japan is aging at a faster rate than in other countries in the world (11). It is speculated that the

number of patients with late-onset ALS will increase even more in the future. The present study evaluated the clinical features in a small number of patients with ALS in Japan. By using ΔFS, we confirmed the result of previous reports.

In conclusion, by using ΔFS, we found that patients with late-onset ALS showed more rapid disease progression than those with early-onset ALS. We propose that ΔFS may be useful for the assessment of affected patients. A larger population is required to validate our conclusion.

The authors state that they have no Conflict of Interest (COI).

References

1. Sabatelli M, Madia F, Conte A, et al. Natural history of young-adult amyotrophic lateral sclerosis. Neurology **71**: 876-881, 2008.
2. Neilson S, Robinson I, Nymoen EH. Longitudinal analysis of amyotrophic lateral sclerosis mortality in Norway, 1966-1989: evidence for a susceptible subpopulation. J Neurol Sci **122**: 148-154, 1994.
3. Neilson S, Gunnarsson LG, Robinson I. Rising amyotrophic lateral sclerosis mortality in France 1968-1990: increased life expectancy and inter-disease competition as an explanation. J Neurol **241**: 448-455, 1994.
4. Neilson S, Gunnarsson LG, Robinson I. Rising mortality from motor neurone disease in Sweden 1961-1990: the relative role of increased population life expectancy and environmental factors. Acta Neurol Scand **90**: 150-159, 1994.
5. McGuire V, Longstreth WT Jr, Koepsell TD, van Belle G. Incidence of amyotrophic lateral sclerosis in three counties in western Washington state. Neurology **47**: 571-573, 1996.
6. Piao YS, Wakabayashi K, Kakita A, et al. Neuropathology with clinical correlations of sporadic amyotrophic lateral sclerosis: 102 autopsy cases examined between 1962 and 2000. Brain Pathol **13**: 10-22, 2003.
7. Traynor BJ, Codd MB, Corr B, Forde C, Frost E, Hardiman O. Incidence and prevalence of ALS in Ireland, 1995-1997: a population-based study. Neurology **52**: 504-509, 1999.
8. Piemonte, Valle d'Aosta. Register for Amyotrophic Lateral Sclerosis (PARALS). Incidence of ALS in Italy: evidence for a uniform frequency in Western countries. Neurology **56**: 239-244, 2001.
9. Sorenson EJ, Stalker AP, Kurland LT, Windebank AJ. Amyotrophic lateral sclerosis in Olmsted County, Minnesota, 1925 to 1998. Neurology **59**: 280-282, 2002.
10. Logroscino G, Beghi E, Zoccolella S, et al. SLAP Registry. Incidence of amyotrophic lateral sclerosis in southern Italy: a population based study. J Neurol Neurosurg Psychiatry **76**: 1094-1098, 2005.
11. Ezrati M. Japan's aging economics. Foreign Aff **76**: 96-104, 1997.
12. Cedarbaum JM, Stambler N, Malta E, et al. BDNF ALS Study Group (Phase III). The ALSFRS-R: a revised ALS functional rating scale that incorporates assessments of respiratory function. J Neurol Sci **169**: 13-21, 1999.
13. Kimura F, Fujimura C, Ishida S, et al. Progression rate of ALSFRS-R at time of diagnosis predicts survival time in ALS. Neurology **66**: 265-267, 2006.
14. Brooks BR. El Escorial World Federation of Neurology criteria for the diagnosis of amyotrophic lateral sclerosis. Subcommittee on Motor Neuron Diseases/Amyotrophic Lateral Sclerosis of the World Federation of Neurology Research Group on Neuromuscular Diseases and the El Escorial "Clinical limits of amyotrophic lateral sclerosis" workshop contributors. J Neurol Sci **124**(suppl): 96-107, 1994.
15. Norris F, Shepherd R, Denys E, et al. Onset, natural history and outcome in idiopathic adult motor neuron disease. J Neurol Sci **118**: 48-55, 1993.
16. Terao S, Li M, Hashizume Y, Mitsuma T, Sobue G. No transneuronal degeneration between human cortical motor neurons and spinal motor neurons. J Neurol **246**: 61-62, 1999.
17. Seljeseth YM, Vollset SE, Tysnes OB. Increasing mortality from amyotrophic lateral sclerosis in Norway? Neurology **55**: 1262-1266, 2000.
18. Forbes RB, Colville S, Swingler RJ. Scottish ALS/MND Register. The epidemiology of amyotrophic lateral sclerosis (ALS/MND) in people aged 80 or over. Age Ageing **33**: 131-134, 2004.
19. Shimohata T, Yanagawa K, Tanaka K, Nishizawa M. Longitudinal analysis of age at onset and initial symptoms in patients with amyotrophic lateral sclerosis. Rinsho Shinkeigaku (Clin Neurol) **46**: 377-380, 2006 (in Japanese, Abstract in English).

J Neurol
DOI 10.1007/s00415-011-6372-7

ORIGINAL COMMUNICATION

Is there delayed gastric emptying in patients with multiple system atrophy? An analysis using the ^{13}C-acetate breath test

Yuji Tanaka · Tomohiro Kato · Hiroshi Nishida · Megumi Yamada · Akihiro Koumura · Takeo Sakurai · Yuichi Hayashi · Akio Kimura · Isao Hozumi · Hiroshi Araki · Masahiko Murase · Masahito Nagaki · Hisataka Moriwaki · Takashi Inuzuka

Received: 26 September 2011 / Revised: 5 December 2011 / Accepted: 10 December 2011

Abstract Autonomic failure is one of the criteria according to the second consensus statement for the diagnosis of multiple system atrophy (MSA). Gastrointestinal symptoms are frequent complaints in patients with MSA and may be associated with reduced gastrointestinal motility due to autonomic nervous system dysfunction. However, there are few reports on gastric emptying in patients with MSA. We investigated gastric emptying in 25 patients with MSA, 20 patients with sporadic adult-onset ataxia of unknown etiology (SAOA), and 20 healthy volunteers using the ^{13}C-acetate breath test. Gastric emptying function is estimated by this test as the half-emptying time (HET) and peak time of the ^{13}C-%-dose-excess curve (T_{max}), with expirations collected for 4 h after a test meal and determination of $^{13}CO_2$ content using an infrared (IR) spectrophotometer. The HET and T_{max} of gastric emptying were significantly delayed in patients with MSA as compared to those in SAOA and controls ($p < 0.01$). The HET and T_{max} were not significantly different between SAOA and controls. No correlation existed between the HET or T_{max} and the duration or severity of the disease in MSA patients. These results suggested that gastric emptying was significantly delayed in patients with MSA, and the delay already appeared in the early stage of the disease. Delayed gastric emptying is one of the autonomic failures and may be a clinical marker of MSA.

Keywords Multiple system atrophy · Sporadic adult-onset ataxia of unknown etiology · Gastric emptying · ^{13}C-Acetate breath test · Autonomic failure

Introduction

Autonomic failure is one of the criteria according to the second consensus statement for the diagnosis of multiple system atrophy (MSA) [1]. Autonomic failure of MSA involves urinary incontinence or orthostatic hypotension [1]. Gastrointestinal symptoms are frequent complaints of patients with MSA and may be associated with reduced gastrointestinal motility due to autonomic nervous system dysfunction [2]. There is a report of gastric emptying (GE) in a small number of patients with MSA [2]. Furthermore, there is no report on the correlation between GE and duration and severity of the disease. Thus, the clinical feature of GE in patients with MSA remains largely unknown.

Recently, the ^{13}C-acetate breath test (^{13}C-ABT) has been widely recognized as useful for evaluating GE because it is less invasive than isotope or acetaminophen methods [3]. In particular, the ^{13}C-ABT is a reliable and non-invasive tool for the analysis of GE rates of liquid phases without radiation exposure [4]. In this study, we used ^{13}C-ABT to compare the GE among patients with MSA, those with sporadic adult-onset ataxia of unknown etiology (SAOA), and healthy volunteers.

Y. Tanaka (✉) · H. Nishida · M. Yamada · A. Koumura · T. Sakurai · Y. Hayashi · A. Kimura · I. Hozumi · T. Inuzuka
Department of Neurology and Geriatrics,
Graduate School of Medicine, Gifu University,
1-1 Yanagido, Gifu City,
Gifu Prefecture 501-1194, Japan
e-mail: yutanaka-gif@umin.net

Y. Tanaka · T. Kato · H. Nishida · H. Araki · M. Murase · M. Nagaki · H. Moriwaki
First Department of Internal Medicine,
Graduate School of Medicine, Gifu University,
1-1 Yanagido, Gifu City,
Gifu Prefecture 501-1194, Japan

Published online: 05 January 2012

Methods

Patients

Our study population consisted of 25 patients with MSA with predominant cerebellar ataxia (MSA-C), 20 patients with SAOA, and 20 healthy volunteers (control group). The patients with MSA-C were diagnosed on the basis of the second consensus statement for the diagnosis of MSA [1]. Those with SAOA were diagnosed according to the criteria of Abele [5, 6]. Furthermore, the patients with MSA-C and those with SAOA were examined by magnetic resonance imaging (1.5 Tesla).

The control group consisted of ten men and ten women; median age was 69.0 years (range 63–73 years). The group of patients with MSA consisted of 12 men and 13 women; median age was 66 years (range 53–81 years); disease duration was 3.0 years (range 0.5–7.3 years). The group of patients with SAOA was composed of nine men and 11 women; median age was 65 years (range 54–73 years); disease duration was 2.5 years (range 1.2–3.6 years) (Table 1). Each group of patients with MSA and SAOA was consecutively consulted at our hospital. None of the MSA and SAOA patients had basic diseases such as liver dysfunction, renal failure, cardiopulmonary disease, diabetes mellitus, gastrointestinal disease, or history of gastric surgery. None of the MSA and SAOA patients takes medication, which might affect gastric motility. Clinical characteristics (including age, gender, and body mass index) were not significantly different among the patients with MSA, those with SAOA, and the control group. The patients with SAOA had no gastrointestinal symptoms. The results of blood examinations were within the normal range. In addition, there were no differences between the patients with MSA and those with SAOA in terms of pepsinogen I, II, and serum gastrin levels, which might affect gastric motility [7]. The positive ratio of anti-*Helicobacter pylori* (HP) antibody did not differ significantly between the patients with MSA and those with SAOA.

Disease stages were defined as follows: stage 0, no gait difficulties, stage 1, disease onset, as defined by onset of gait difficulties, stage 2, loss of independent gait, as defined by permanent use of a walking aid or reliance on a supporting arm, stage 3, confinement to wheelchair, as defined by permanent use of a wheelchair [6]. In MSA with stage 0 there were five patients (20%), in stage 1, there were seven patients (28%), in stage 2, eight patients (32%), and in stage 3, there were five patients (20%). In SAOA with stage 0, there were six patients (30%), in stage 1, there were six patients (30%), in stage 2, there were five patients (25%), and in stage 3, there were three patients (15%).

Informed consent was obtained from each subject prior to participation in this study. The study protocol was approved by the Ethical Committee of Gifu University, and was carried out in accordance with the 1975 Declaration of Helsinki.

Gastric emptying examination

The GE examination was carried out using the ^{13}C-breath test according to Ghoos [3] with slight modifications. MSA patients, SAOA patients, and healthy volunteers were tested after an overnight fast of 12 h. None of the MSA and SAOA patients took medication for digestive tract function for 24 h. Early in the morning, MSA patients, SAOA patients, and healthy volunteers took a liquid test meal (Racol: TM 200 kcal/200 ml; Otsuka Pharmaceuticals Co., Ltd., Tokyo, Japan) containing 100 mg ^{13}C-sodium acetate. Thereafter, an expiration breath sample was collected every 10 min for 4 h and analyzed for $^{13}CO_2$ using an infrared (IR) spectrophotometer (UBiT-IR300; Otsuka Electronics Co., Ltd., Tokyo, Japan). All subjects were in a sitting position during the examination.

The principle of the ^{13}C-ABT is ingestion of a liquid test meal containing ^{13}C-acetate, GE, absorption from the digestive tract, metabolism in the liver (production of $^{13}CO_2$), and expiration from the lung, which results in an increase in $^{13}CO_2$ in the expired breath [8, 9].

Table 1 Clinical characteristics of patients with multiple system atrophy and those with sporadic adult-onset ataxia of unknown etiology

	Controls (n = 20)	MSA (n = 25)	SAOA (n = 20)	p value
Age (years)	69 (63–73)	66 (53–81)	65 (54–73)	0.072
Gender (male/female)	10/10	12/13	9/11	0.950
BMI (kg m^{-2})	18.7 (16.7–23.8)	20.0 (13.2–28.9)	20.7 (16.7–26.5)	0.078
Duration (years)		3.0 (0.5–7.3)	2.5 (1.2–6.0)	0.664

Variables are expressed as median (range). Categorical variables were compared using the Chi-square test. Medians were compared using the Kruskal–Wallis test

MSA multiple system atrophy, *SAOA* sporadic adult-onset ataxia of unknown etiology, *BMI* body mass index

Mathematical analysis

The data were used for mathematical curve fitting. A best-fit curve of expired $^{13}CO_2$ was constructed for each subject. The percentage-$^{13}CO_2$ cumulative excretion in the breath was assessed using a nonlinear regression formula [10, 11] $y = m\ (1-e^{-kt})^{\beta}$ to fit the curve of the cumulative ^{13}C recovery. The percentage of $^{13}CO_2$ excretion per hour was fitted to the formula $mk\beta e^{-kt}\ (1-e^{-kt})^{\beta-1}$, t is time and m, k, and β are constants. The value of m represents the total cumulative $^{13}CO_2$ recovery when the time is infinite. The half-emptying time (HET) was calculated using the formula HET $= -1/k$ ln $(1-e^{-1/\beta})$. T_{max} is the peak time of the ^{13}C-%-dose-excess curve (%-dose/h) based on a time profile of the $^{13}CO_2$ excretion rate. The parameters were estimated with the Excel software (Microsoft, Redmond, WA).

Statistical analysis

Categorical variables were compared using the Chi-square test. Other variables were expressed as median (range). Between two groups, medians were compared using the Mann–Whitney U test. Between three groups, medians were compared using the Kruskal–Wallis test. Paired two groups were analyzed using the Spearman's correlation coefficient by rank. All analyses were carried out on StatView statistical software, version 5.0 (Abacus Concepts, Inc., Berkeley, CA). A p value of less than 0.05 was considered significant.

Results

T_{max} in MSA, SAOA, and controls

The examinations were safely carried out in all MSA patients, SAOA patients, and controls. T_{max} was significantly delayed in MSA patients (median 1.50 h, range 0.83–2.67 h) as compared with the controls (median 0.83 h, range 0.67–1.00 h) ($p < 0.01$) or with SAOA patients (median 0.83 h, range 0.50–1.67 h) ($p = 0.01$) (Fig. 1). There was no significant difference in T_{max} between SAOA and controls.

HET in MSA, SAOA, and controls

The HET was significantly delayed in MSA patients (median 2.77 h, range 1.67–3.71 h) as compared to the controls (median 1.44 h, range 1.30–1.64 h) ($p < 0.01$) or with SAOA patients (median 1.54 h, range 1.30–3.09 h) ($p = 0.01$) (Fig. 2). There was no significant difference in HET between SAOA and controls (Fig. 2).

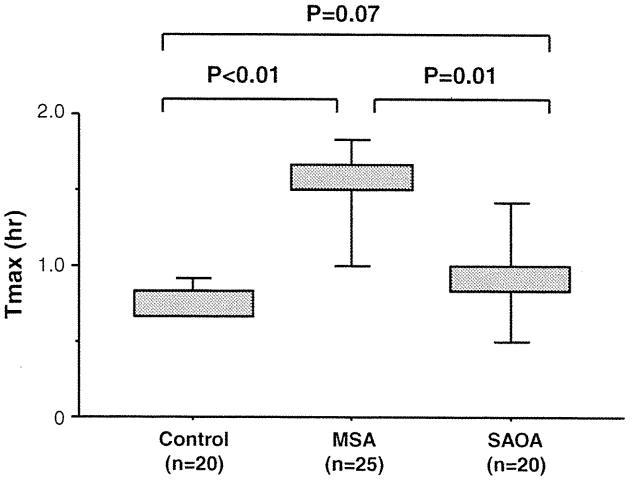

Fig. 1 Peak time of the ^{13}C-%-dose-excess curve (T_{max}) in controls, patients with multiple system atrophy (*MSA*), and those with sporadic adult-onset ataxia of unknown etiology (*SAOA*)

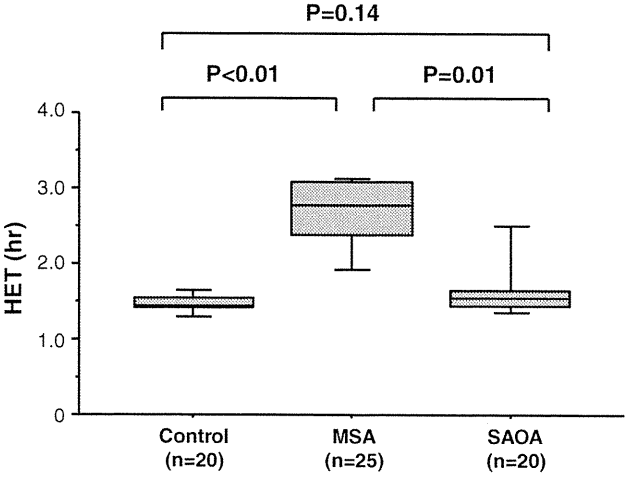

Fig. 2 Half-emptying time (*HET*) in controls, patients with multiple system atrophy (*MSA*), and those with sporadic adult-onset ataxia of unknown etiology (*SAOA*)

Correlation between GE and disease stage in MSA

In patients with MSA, either T_{max} ($p = 0.89$) or HET of GE using the ^{13}C-ABT did not correlate with the severity of the disease ($p = 0.95$). Neither T_{max} ($p = 0.70$) nor HET correlate with the duration of the disease ($p = 0.70$).

Discussion

In the present study, we have shown two novel important points. First, our results showed that GE is significantly delayed in patients with MSA as compared to patients with SAOA and controls. Second, GE of patients with MSA is already delayed in the early stage of the disease.

Autonomic failure is one of the criteria according to the second consensus statement for the diagnosis of MSA [1]. Among lower gastrointestinal symptoms, constipation is a common feature and a change in bowel habits suggests autonomic involvement of the lower gut [12]. Patients with MSA sometimes complain of upper gastrointestinal symptoms [2]. Gastrointestinal symptoms may be associated with reduced gastrointestinal motility due to autonomic nervous system dysfunction of MSA [2]. The previous study suggested that GE of patients with MSA was slower than the control [2]. However, it was not clear whether GE of MSA patients correlated duration and severity of the disease. In this study, we demonstrated that GE of patients with MSA is already delayed from the early stage.

With respect to the pathological background of MSA, previous studies have supported the presence of a central lesion. The pathological lesions of autonomic failure are defined by loss of preganglionic neurons of the thoracic intermediolateral column (IML) and sacral IML, and by loss of visceromotor neurons of Onuf's nuclei in the sacral segment [13]. The dorsal motor nuclei of the vagus are also involved [13]. Moreover, involvement of the hypothalamus has been reported [14–16]. Interestingly, a recent study demonstrated accumulation of phosphorylated alpha-synuclein in the peripheral sympathetic ganglia in two out of eight patients with MSA [17]. Furthermore, neurohormonal dysfunction is also a frequent co-morbidity in patients with MSA, and the determination of the pathological involvement of the autonomic neurons, which are responsible for circadian rhythms and responses to stress, provides new insights into autonomic failure and neurohormonal dysfunction in MSA [18]. It is reported that patients with MSA have an impaired circadian rhythm of gastric myoelectrical activity due to the degeneration of the central autonomic neurons [19]. The pathological lesions of gastrointestinal failure in MSA patients might correlate both upper and lower gastrointestinal functions. These mechanisms might affect the delayed GE in MSA.

As of now, and with regard to lower gastrointestinal symptoms, constipation is considered one of the most common manifestations of autonomic dysfunction in MSA, occurring in 33% of patients [20, 21]. Patients with MSA complain of constipation at a relatively early stage of the disease [22]. Furthermore, the rectal sphincter in MSA is frequency-denervated because of degeneration of Onuf's nuclei in the sacral cord [23]. The electromyogram of the rectal sphincter may be abnormal [24]. Involvement of Onuf's nuclei in MSA is time-dependent [25]. This may represent a somatic, but not an autonomic, dysfunction [26].

In some patients with non-hereditary degenerative adult-onset ataxia at an early stage, it is difficult to distinguish between MSA and SAOA. Inclusion criteria of SAOA were as follows: (1) progressive ataxia, (2) disease onset after the age of 20 years, (3) informative and negative family history, (4) no established symptomatic cause, (5) no subacute onset of ataxia, (6) negative molecular genetic testing for SCA, and (7) no possible or probable MSA according to established clinical criteria [5, 6]. Although the neuropathological difference between MSA and SAOA is not clear, the difference in clinical features between patients with MSA and those with SAOA was reported [5]. However, there were scant data of gastrointestinal symptoms in patients with SAOA [5]. Hence, we compared GE of patients with MSA and those with SAOA. In this study, we showed that GE was significantly delayed in patients with MSA as compared to patients with SAOA. The delayed GE may be one of the markers to be useful to explain the difference between patients with MSA and those with SAOA.

In conclusion, our study demonstrated that GE is significantly delayed in MSA patients as compared to SAOA patients and controls, and that no correlation existed between GE of MSA patients and duration and severity of the disease. From the viewpoint of an early diagnosis, it will be important to actually measure GE in MSA patients in clinical settings. Our results demonstrated that GE is already delayed at the early stage of MSA. Therefore, we speculate that delayed GE is one of the autonomic failures of MSA and may be one of the markers for MSA.

Conflicts of interest None.

References

1. Gilman S, Wenning GK, Low PA, Brooks DJ, Mathias CJ, Trojanowski JQ, Wood NW, Colosimo C, Dürr A, Fowler CJ, Kaufmann H, Klockgether T, Lees A, Poewe W, Quinn N, Revesz T, Robertson D, Sandroni P, Seppi K, Vidailhet M (2008) Second consensus statement on the diagnosis of multiple system atrophy. Neurology 71:670–676
2. Thomaides T, Karapanayiotides T, Zoukos Y, Haeropoulos C, Kerezoudi E, Demacopoulos N, Floodas G, Papageorgiou E, Armakola F, Thomopoulos Y, Zaloni I (2005) Gastric emptying after semi-solid food in multiple system atrophy and Parkinson disease. J Neurol 252:1055–1059
3. Ghoos YF, Maes BD, Geypens BJ, Mys G, Hiele MI, Rutgeerts PJ, Vantrappen G (1993) Measurement of gastric emptying rate of solids by means of a carbon-labeled octanoic acid breath test. Gastroenterology 104:1640–1647
4. Braden B, Adams S, Duan LP, Orth KH, Maul FD, Lembcke B, Hör G, Caspary WF (1995) The ^{13}C-acetate breath test accurately reflects gastric emptying of liquids in both liquid and semisolid test meals. Gastroenterology 108:1048–1055
5. Abele M, Bürk K, Schöls L, Schwartz S, Besenthal I, Dichgans J, Zühlke C, Riess O, Klockgether T (2002) The aetiology of sporadic adult-onset ataxia. Brain 125:961–968
6. Abele M, Minnerop M, Urbach H, Specht K, Klockgether T (2007) Sporadic adult-onset ataxia of unknown etiology: a clinical, electrophysiological and imaging study. J Neurol 254:1384–1389

7. Yoshihara M, Sumii K, Haruma K, Kiyohira K, Hattori N, Kitadai Y, Komoto K, Tanaka S, Kajiyama G (1998) Correlation of ratio of serum pepsinogen I and II with prevalence of gastric cancer and adenoma in Japanese subjects. Am J Gastroenterol 93:1090–1096
8. Tanaka Y, Kato T, Nishida H, Araki H, Murase M, Nagaki M, Moriwaki H, Inuzuka T (2009) Is there a difference in gastric emptying between Parkinson's disease patients under long-term L-dopa therapy with and without motor fluctuations? An analysis using the ^{13}C-acetate breath test. J Neurol 256:1972–1976
9. Tanaka Y, Kato T, Nishida H, Yamada M, Koumura A, Sakurai T, Hayashi Y, Kimura A, Hozumi I, Araki H, Murase M, Nagaki M, Moriwaki H, Inuzuka T (2011) Is there a delayed gastric emptying of patients with early-stage, untreated Parkinson's disease? An analysis using the ^{13}C-acetate breath test. J Neurol 258:421–426
10. Gatti C, di Abriola FF, Dall'Oglio L, Villa M, Franchini F, Amarri S (2000) Is the ^{13}C-acetate breath test a valid procedure to analyse gastric emptying in children? J Pediatr Surg 35:62–65
11. Gonza'lez A, Mugueta C, Parra D, Labayen I, Martinez A, Varo N, Monreal I, Gil MJ (2000) Characterisation with stable isotopes of the presence of a lag phase in the gastric emptying of liquids. Eur J Nutr 39:224–228
12. Mathias CJ (2006) Multiple system atrophy and autonomic failure. J Neural Transm 70:343–347
13. Yoshida M (2007) Multiple system atrophy: alpha-synuclein and neural degeneration. Neuropathology 27:484–493
14. Tsai A, Maehara K, Iizuka R (1992) Loss of catecholaminergic neuron in the hypothalamus of multiple system atrophy. Rinsho Shinkeigaku 32:125–130 (in Japanese with English abstract)
15. Nakamura S, Ohnishi K, Nishimura M, Suenaga T, Akiguchi I, Kimura J, Kimura T (1996) Large neurons in the tuberomammillary nucleus in patients with Parkinson's disease and multiple system atrophy. Neurology 46:1693–1696
16. Ozawa T, Oyanagi K, Tanaka H, Horikawa Y, Takahashi H, Morita T, Tsuji S (1998) Suprachiasmatic nucleus in a patient with multiple system atrophy with abnormal circadian rhythm of arginine-vasopressin secretion into plasma. J Neurol Sci 154: 116–121
17. Nishie M, Mori F, Fujiwara H, Hasegawa M, Yoshimoto M, Iwatsubo T, Takahashi H, Wakabayashi K (2004) Accumulation of phosphorylated alpha-synuclein in the brain and peripheral ganglia of patients with multiple system atrophy. Acta Neuropathol 107:292–298
18. Ozawa T (2007) Morphological substrate of autonomic failure and neurohormonal dysfunction in multiple system atrophy: impact on determining phenotype spectrum. Acta Neuropathol 114:201–211
19. Suzuki A, Asahina M, Ishikawa C, Asahina KM, Honma K, Fukutake T, Hattori T (2005) Impaired circadian rhythm of gastric myoelectrical activity in patients with multiple system atrophy. Clin Auton Res 15:368–372
20. Stefanova N, Bücke P, Duerr S, Wenning GK (2009) Multiple system atrophy: an update. Lancet Neurol 8:1172–1178
21. Colosimo C (2011) Nonmotor presentations of multiple system atrophy. Nat Rev Neurol 7:295–298
22. Mabuchi N, Hirayama M, Koike Y, Watanabe H, Ito H, Kobayashi R, Hamada K, Sobue G (2005) Progression and prognosis in pure autonomic failure (PAF): comparison with multiple system atrophy. J Neurol Neurosurg Psychiatry 76:947–952
23. Bennett T (1983) Physiological investigation of diabetic autonomic failure. In: Bannister R (ed) Autonomic failure. Oxford University Press, Oxford, pp 407–436
24. Ravits J, Hallett M, Nilsson J, Polinsky R, Dambrosia J (1996) Electrophysiological tests of autonomic function in patients with idiopathic autonomic failure syndromes. Muscle Nerve 19: 758–763
25. Yamamoto T, Sakakibara R, Uchiyama T, Liu Z, Ito T, Awa Y, Yamamoto K, Kinou M, Yamanishi T, Hattori T (2005) When is Onuf's nucleus involved in multiple system atrophy? A sphincter electromyography study. J Neurol Neurosurg Psychiatry 76: 1645–1648
26. Ravits JM (1997) AAEM minimonograph #48: autonomic nervous system testing. Muscle Nerve 20:919–937

L-MPZ, a Novel Isoform of Myelin P0, is Produced by Stop Codon Readthrough*

Yoshihide Yamaguchi[1], Akiko Hayashi[1], Celia W. Campagnoni[2†], Akio Kimura[3], Takashi Inuzuka[3], and Hiroko Baba[1]

[1]Department of Molecular Neurobiology, Tokyo University of Pharmacy and Life Sciences, Hachioji, Tokyo 192-0392, Japan

[2]Semel Institute for Neuroscience and Human Behavior, University of California at Los Angeles, Los Angeles, California 90095
[†]Deceased

[3]Department of Neurology and Geriatrics, Gifu University, Graduate School of Medicine, Gifu 501-1194, Japan

*Running title: *L-MPZ is a novel isoform of P0*

To whom correspondence should be addressed: Yoshihide Yamaguchi, Department of Molecular Neurobiology, Tokyo University of Pharmacy and Life Sciences, 1432-1 Horinouchi, Hachioji, Tokyo 192-0392, Japan, Tel.: +81 (42) 676-3040; Fax: +81 (42) 676-3040; E-mail: yoshiy@toyaku.ac.jp

Keywords: myelin; neuropathy; stop codon readthrough

Background: The structure and function of myelin P0-related 36-kDa protein are totally unknown.
Result: A novel isoform of P0, L-MPZ, contains extra C-terminus derived from 3'UTR of P0 mRNA and is expressed in peripheral myelin.
Conclusion: L-MPZ is produced by stop codon readthrough and probably related with peripheral myelinogenesis.
Significance: Analyses of L-MPZ are crucial for understanding readthrough mechanism in mammals and myelinogenesis.

SUMMARY

Myelin protein zero (P0 or MPZ) is a major myelin protein (~30 kDa) expressed in the peripheral nervous system (PNS) in terrestrial vertebrates. Several groups have detected a P0-related 36-kDa (or 35-kDa) protein that is expressed in the PNS as an antigen for the serum IgG of patients with neuropathy. The molecular structure and function of this 36-kDa protein are, however, still unknown. We hypothesized that the 36-kDa protein may be derived from P0 mRNA by stop codon readthrough. We found a highly conserved region after the regular stop codon in predicted sequences from the 3'UTR of P0 in higher animals. MS of the 36-kDa protein revealed that both P0 peptides and peptides deduced from the P0 3'UTR sequence were found among the tryptic fragments. In transfected cells and in an *in vitro* transcription/translation system, the 36-kDa molecule was also produced from the identical mRNA that produced P0. We designated this 36-kDa molecule as large myelin protein zero (L-MPZ), a novel isoform of P0 that contains an additional domain at the C terminus. In the PNS, L-MPZ was localized in compact myelin. In transfected cells, just like P0, L-MPZ was localized at cell-cell adhesion sites in the plasma membrane. These results suggest that L-MPZ produced by the stop codon readthrough mechanism is potentially involved in myelination. Since this is the first finding of stop codon readthrough in a common mammalian protein, detailed analysis of L-MPZ expression will help to understand the mechanism of stop codon readthrough in mammals.

Peripheral myelin protein zero (known as P0 or MPZ) is a type I transmembrane adhesion

molecule, which belongs to the immunoglobulin (Ig) superfamily and constitutes >50% of the total peripheral nervous system (PNS) myelin protein in vertebrates (1). The P0 gene encodes a protein of 248 amino acids (aa) including a 29-aa signal sequence. Mature P0 protein (219 aa) is N-glycosylated and has an apparent molecular weight of ~30 kDa. Homophilic interactions between the extracellular Ig domain lead to tight adhesion between each layer in PNS myelin (2). The highly basic intracellular domain of P0 is required for compaction of the cytoplasmic side of myelin and is also involved in extracellular adhesion (3, 4). The P0 gene consists of six exons, and protein sequences are evolutionarily highly conserved from fish to humans (1). In particular, sequences from mouse, rat, bovine, and human have >90% identity. Thus, P0 is important for the function of the PNS, and a large number of P0 mutations cause hereditary motor sensory neuropathies (5).

Several groups have suggested that a 36-kDa (or 35-kDa) autoantigen that reacted with sera from patients with neuropathies may be involved in various neuropathies. This molecule has an identical N-terminal aa sequence and partial internal sequence as P0 (6-9), but the size of this protein is somewhat larger than P0. Although there are three truncated, spliced variants of P0 that are related to the omission or partial skipping of exon 3 (10), no other mRNA transcripts have been reported. Ishida et al. (8) screened a human sciatic nerve (ScN) cDNA expression library using a serum sample obtained from a patient and found that three positive clones included small cDNA fragments matching part of the 3′UTR of P0. The molecular structure and function of this protein are, however, totally unknown.

Translation termination is a crucial step that controls expression during protein synthesis. During this process, well-regulated stop codon readthrough is a mechanism that is thought to expand the coding potential of a limited genome in viruses (11), yeasts (for review, 12), and *Drosophila* (13-15). It is believed that this mechanism occurs in higher animals and that it can have substantial effects on the function of the encoded protein and on the phenotype of the cell. Rabbit β -globin is, however, the only reported example of the utilization of this mechanism in a higher organism (16, 17).

Here we show that the neuropathy-associated 36-kDa protein is a novel form of P0 that is produced by translational stop codon readthrough. We designated this protein as large myelin protein zero (L-MPZ).

EXPERIMENTAL PROCEDURES

Serum samples–Serum that was positive for antibodies against the 36-kDa protein was obtained from a 54-year-old female patient with chronic inflammatory demyelinating polyneuropathy (CIDP) at Gifu University Hospital and was stored in aliquots at −80°C until use. Normal serum was obtained from a 62-year-old female volunteer and was stored in aliquots at −80°C until use. This study was approved by the Tokyo University of Pharmacy and Life Sciences Review Committee and the Gifu University Review Committee. The patient and a volunteer provided written informed consent prior to participation in the study.

Animals–Wistar rats that were 8 weeks old and postnatal day (P)1, P3, P5, and P7 Wistar rats were purchased from Japan SLC (Hamamatsu, Japan). All experiments were conducted in accordance with the guidelines on the care and use of animals of the Tokyo University of Pharmacy and Life Sciences Animal Use Committee.

Preparation of brain and ScN homogenates–A homogenate was prepared from 10 8-week-old male Wistar rats. All procedures were carried out on ice or at 4°C. Homogenates were obtained as described (18) with slight modification. Briefly, ScNs were dissected and snap frozen in liquid nitrogen. The frozen tissues were then ground into powder using a mortar and homogenized with a homogenizer (Heidolph, Schwabach, Germany) in nine volumes (w/v) of 0.32 M sucrose containing 5 mM Tris-HCl, pH 7.5; 2 mM EGTA; 0.75 μM aprotinin; 1 μM leupeptin; 1 μM pepstatin A; and 0.4 mM PMSF (Homogenization Buffer). To remove chromosomal DNA, cell debris, and fibers, the homogenates were centrifuged at 500 × *g* for 10 min, and the supernatants were collected and stored as a whole homogenate fraction at −80°C. The protein concentration was determined using a bicinchoninic acid assay (Pierce Biotechnology, Rockford, IL, USA).

Isolation of membrane, cytosol, and myelin fractions from ScN homogenates–Whole ScN homogenate was collected and centrifuged for 30

min at 200,000 × *g*. The supernatant collected at this stage contained the cytosolic fraction. The precipitate, which was the membrane fraction, was then re-homogenized in Homogenization Buffer. These fractions were stored at −80°C. The myelin fraction was purified as described (18).

Western blot analysis–Western blot analysis using SDS-PAGE and two-dimensional gel electrophoresis (2DE) with a cationic detergent, cetyltrimethylammonium bromide (CTAB), was performed as described (18). This 2DE method using cationic detergent is appropriate for the analysis of highly hydrophobic membrane proteins, especially those in myelin (18, 19). CTAB-2DE is advantageous for the solubilization of hydrophobic proteins. The primary antibodies used in western blotting are described below.

Peptide absorption of immunoreactivity–Immunoreactivity of the serum IgG in western blotting was blocked by peptide absorption. The absorption peptides were synthesized by GenScript (Piscataway, NJ, USA). Appropriate concentrations of the serum and antibody were incubated overnight at 4°C with each of the synthetic peptides (20 μg/ml) in a solution containing 0.15 M NaCl and 20 mM Tris-HCl, pH 7.5 (TBS). This mixture was diluted 1:9 (v/v) in 0.3% skim milk/0.1% Tween-20/TBS and was used as the primary antibody solution for western blotting.

Deglycosylation–Peptide:*N*-glycosidase F (PNGase F, EC 3.5.1.52) digestion of the peptide was performed as described (20) with slight modification. Briefly, the samples were boiled for 5 min in 0.5% SDS and 100 mM 2-mercaptoethanol and cooled to room temperature. Triton X-100 (10%) was added to a final concentration of 2.5%, and the sample was diluted to 1 μg/ml protein by adding 0.1 M phosphate buffer (PB), pH 6.8, and 25 mM EDTA. The mixture was incubated with 0.25 U PNGase F (Roche)/30 μg protein for 15 h at 30°C. The deglycosylated samples were analyzed by western blotting.

MS analysis–PNS myelin proteins were separated with CTAB-2DE and visualized with fluorescent staining (18, 21). The excised 36-kDa spot was analyzed by the Pasarow Mass Spectrometry Laboratory at the University of California at Los Angeles. Tryptic peptide fractions from HPLC chromatography were loaded into nano-electrospray emitters (Proxeon; Thermo, San Jose, CA, USA) for immediate analysis using a nano-electrospray source–equipped mass spectrometer (LTQ-FT Ultra; Thermo). Identification of tryptic peptides from P0 and predicted L-MPZ–specific sequences was achieved by analyzing MS/MS spectra obtained using an MS/MS ion search of the Mascot Server (Matrix Science, Boston, MA, USA).

Plasmid constructs–Human P0 cDNA in the pUC19 vector (22) was a gift from Dr. Kiyoshi Hayasaka (Yamagata University, Yamagata, Japan). The *Eco*RI restriction fragment of full-length P0 was cloned into the *Eco*RI site of the pcDNA3.0 vector (Invitrogen, Carlsbad, CA, USA), which contains a CMV promoter for expression in mammalian cell culture (hP0/pcDNA3). Mutants of deletion (del-L-MPZ/pcDNA3) or replacements [TAG → GCG, Ala (MutA-L-MPZ/pcDNA3); TAG → TAC, Tyr (MutY-L-MPZ/pcDNA3)] of P0 stop codon, mutant of 3'UTR-deletion just after P0 stop codon (P0-3'del/pcDNA3), and mutant of frame shift mutation by deletion of single base pair immediately after P0 stop codon (P0_only/pcDNA3) were generated from hP0/pcDNA3 using the PrimeSTAR Mutagenesis Basal kit (Takara Bio, Otsu, Japan) (Fig. 9B).

Cell culture and electroporation–Monolayers of HeLa and NIH/3T3 cells were maintained in DMEM (GIBCO-BRL/Invitrogen) supplemented with 10% FBS in 5% CO_2 at 37°C. Transfection of pcDNA3.0 (empty vector) or hP0/pcDNA3 was performed with an electroporator (MicroPorator, DigitalBio; now provided as Neon by Invitrogen) according to the manufacturer's instructions (Hela cell, 0.7 μg plasmid DNA in 10 μl solution, 1020 V, 35 ms, two pulses; NIH3T3, 15 μg plasmid DNA in 100 μl solution, 1350 V, 20 ms, two pulses).

Preparation of transfected cell cultures–Transfected NIH/3T3 cells (3×10^6 cells) were plated on a 100-mm culture dish and cultured in 10% FBS/DMEM. Twenty-four hours after plating, the cells were washed with phosphate-buffered saline (PBS) and Homogenization Buffer containing 1 mM DTT. The cells were harvested with a cell scraper and lysed using a syringe with sequential passes through 21-G and 27-G needles. The supernatant was collected by centrifuging at 500 × *g* for 10 min and then used for western blot

analysis. Transfected HeLa cells (5×10^5 cells) were plated onto 18-mm coverslips coated with poly-L-lysine and cultured in 10% FBS/MEM-α containing GlutaMax (GIBCO-BRL/Invitrogen). The cells were used for immunostaining 24 h after plating onto the coverslips.

In vitro translation–*In vitro* translation of P0 and/or L-MPZ from hP0/pcDNA3 was performed with the T_NT Quick Coupled Transcription/Translation System (Promega, Madison, WI, USA) according to the manufacturer's instructions. L-[^{35}S]methionine (EasyTag PerkinElmer, Waltham, MA, USA) was used for labeling of synthesized proteins. The radiolabeled proteins were analyzed by SDS–PAGE followed by autoradiography on BioMax MR films (Kodak, Rochester, NY, USA). For quantification, the intensity of each band was measured by ImageGauge v4.23 (Fujifilm, Tokyo, Japan), and the relative ratio of P0 and L-MPZ with or without G418 was calculated. Values were obtained from four samples. Statistical analysis was performed using a two-way ANOVA (PRISM 5; GraphPad Software, La Jolla, CA USA) followed by Bonferroni multiple comparison test.

Immunostaining–Transfected HeLa cells plated onto coverslips were fixed with 4% paraformaldehyde (PFA) at room temperature (RT) for 10 min and permeabilized for 5 min at RT in 0.1% Triton X-100 in PBS. The coverslips were preincubated for 1 h in 10% normal donkey serum (NDS)/PBS and then incubated overnight at 4°C with primary antibodies diluted in NDS/PBS. After rinsing, the cells were incubated with Alexa Fluor 488– or 594–conjugated secondary antibodies for 1 h at RT. The labeled coverslips were then rinsed and mounted onto glass slides with Vectashield containing DAPI (Vector Laboratories, Burlingame, CA, USA). Images were captured with confocal microscopy (Olympus, Tokyo, Japan).

Frozen sections of the ScN were prepared by transcardial perfusion of 8-week-old Wistar rats with 4% PFA in 0.1 M PB, pH 7.4. The 10-μm-thick frozen sections were permeabilized and blocked for 1 h in TBS containing 0.3% Triton X-100 and 10% NDS (NDS/T-TBS). The sections were then incubated overnight at 4°C with primary antibodies diluted in NDS/T-TBS, thoroughly rinsed in TBS, and incubated with fluorescently labeled secondary antibodies for 1 h at RT. Finally, the labeled frozen sections were rinsed and mounted in Vectashield containing DAPI. The images were captured with confocal microscopy.

Antibodies–The following antibodies were used for immunostaining: goat polyclonal anti-P0 antibody produced against the peptide sequence (DHSRSTKAVSEK) of the C-terminal region of human P0 (1:500; Abnova, Taipei, Taiwan), rat monoclonal anti–myelin basic protein antibody (anti-MBP; 1:200; Chemicon/Millipore, Billerica, MA, USA), mouse monoclonal anti-neurofilament (anti-NF; 1:5; Nichirei, Tokyo, Japan), and rabbit polyclonal anti–L-MPZ (1:4000) antibody, which was produced by immunization with a keyhole limpet hemocyanin–conjugated 21-aa peptide (C-LRPAVKSPSRTSLKNALKNM; synthesized by GenScript) of the human L-MPZ–specific region. The secondary antibodies used for immunostaining were Alexa Fluor 488– and 594–conjugated species-specific antibodies (1:2000; Molecular Probes/Invitrogen). For western blotting, the following antibodies were used: the serum obtained from the patient with CIDP (1:200), goat polyclonal anti-P0 (1:4000), rabbit polyclonal anti–L-MPZ (1:40000), mouse monoclonal anti-β-catenin (1:2,000; BD Biosciences, San Jose, CA, USA), mouse monoclonal anti-actin (1:4,000; Sigma-Aldrich, St. Louis, MO, USA), rabbit polyclonal anti-Glyceraldehyde-3-phosphate dehydrogenase (GAPDH) (1:2000, Imgenex, San Diego, CA), mouse monoclonal anti-paxillin (1:5,000; BD Biosciences), and anti-MBP (1:2000) antibodies. The secondary antibodies used for western blotting were horseradish peroxidase–conjugated anti-mouse, anti–rabbit, anti–rat, anti–goat (1:10000; Jackson ImmunoResearch Laboratories, West Grove, PA, USA), and anti–human IgG (1:5000; American Qualex, San Clemente, CA, USA).

RESULTS

Characterization of the 36-kDa protein recognized by serum IgG from a patient with neuropathy–In the course of investigating neuropathy-associated autoantigens recognized by sera from patients with neuropathy, we found that some sera detected a 36-kDa molecule in rat ScN homogenate. To characterize this 36-kDa protein, western blot analysis was performed using fractions from rat brain and ScN. The 36-kDa

protein was detected only in the whole homogenate fraction from rat ScN and not in brain (Fig. 1A). This 36-kDa protein was detected in the β-catenin (adherence junction marker)-enriched ScN membrane fraction (Fig. 1B), especially in the MBP molecules (myelin marker)-enriched myelin fraction (Fig. 1C). To investigate N-linked glycosylation, western blotting with PNGase F–treated ScN whole homogenate was performed. A deglycosylation assay with PNGase F revealed that both P0 and the 36-kDa protein bands were similarly shifted downward, suggesting that the 36-kDa protein had nearly the same sugar chain content as P0 (Fig. 1D). Thus, the serum from the patient recognized the peptide portion of this PNS myelin protein. These properties corresponded to those of the previously reported 36-kDa (or 35-kDa) protein antigen (6-9). Therefore, this 36-kDa protein is likely to be a common autoantigen in PNS myelin.

To investigate the relationship between this 36-kDa protein and P0, we tested whether anti-P0 antibody recognized the 36-kDa band using commercially available anti-P0 antibody, which recognizes the C-terminal region of human P0. A 36-kDa band was detected by both anti-P0 and the patient serum (Fig. 2A). To investigate whether these 36-kDa molecules were identical, we performed 2DE-western blotting using CTAB, which is suitable for analyzing highly hydrophobic membrane protein spots (18). Proteins from rat ScN homogenates were visualized with silver staining of CTAB-2DE membranes (left panels of Fig. 2B and 2C). The same 36-kDa spots were recognized by both the patient serum and anti-P0 antibody (white arrows in Fig. 2B and 2C). This suggests that the 36-kDa molecule has an antigen in common with the P0 C-terminal region.

Evolutionarily conserved aa sequences derived from the 3′UTR of P0 mRNA—The N-terminal sequence of the 36-kDa (or 35-kDa) band detected by the sera of patients with neuropathy is identical to that of P0, and 36-kDa (or 35-kDa) bands are found in human, bovine, rat, and mouse PNS (6-9). In addition, Ishida et al. (8) showed that only small cDNA fragments containing a partial P0 3′UTR have been obtained by expression cloning of the human ScN cDNA library using the serum from a patient with neuropathy. These data strongly suggest that this protein is a novel isoform of P0 and contains extra aa derived from the 3′UTR of P0 mRNA. Because exon 6 encodes part of the P0 C terminus, the stop codon, and the entire 3′UTR (Fig. 3A), we carefully examined the sequence of the 3′UTR of P0 mRNA. After a typical stop codon (UAG), there were 189 nucleotides before the next in-frame stop codon (UGA) appeared. Evolutionary comparisons of P0 3′UTR cDNAs revealed that the extra 63 predicted aa immediately after the regular stop codon were well conserved from frog (*Xenopus laevis*) to human (Fig. 3A). After the second stop codon, no additional conserved regions were found in the 3′UTR. Interestingly, no such sequence homology was found in zebrafish P0 cDNA (data not shown). In addition, no such conserved aa sequence immediately after the regular stop codon was seen in other common myelin protein genes, including those encoding myelin proteolipid protein (PLP), myelin-associated glycoprotein, MBP, and peripheral myelin protein 22 (data not shown).

To investigate whether the 36-kDa protein actually contains the extra 63 aa, tryptic peptides from the 36-kDa protein spot on CTAB-2DE gels were analyzed by MS. Twelve tryptic peptides from the 36-kDa protein corresponded to the predicted tryptic peptides from P0, and five additional peptides corresponded to the predicted sequence in the P0 3′UTR (Fig. 3B). These peptides covered almost the entire P0 molecule including the N terminus. These data support the possibility that the 36-kDa protein is derived from P0 mRNA.

P0 has a phosphorylation site (RSTK) that is regulated by protein kinase C (PKC)-α in the cytoplasmic C-terminal region (Fig. 3B); this PKC-mediated phosphorylation is necessary for P0-mediated adhesion (4). To look for a possible predicted phosphorylation site in the extra 63 aa, we analyzed this sequence with the NetPhos 2.0 Server (http://www.cbs.dtu.dk/services/NetPhos/). One putative PKC-mediated phosphorylation site (RTSLK; Fig. 3B) was found with a high score.

Elimination of immunoreactivity for the 36-kDa band by the specific peptide derived from the predicted sequence in the 3′UTR of P0 mRNA—To determine whether the extra 63 aa of the 36-kDa protein contain antigenic sites, we performed peptide absorption using synthetic peptides derived from the predicted sequence in the 3′UTR of human P0 mRNA. First, two peptides (Fig. 4A; P0-1 and P0-2) that matched the

predicted extra sequence were synthesized and used for absorption. The immunoreactivity for the 36-kDa band in the patient serum was completely absorbed by the P0-2 peptide but not at all by the P0-1 peptide (Fig. 4B). To further investigate the epitope, five different 12-mer peptides (Fig. 4A; P0-2-1 to -5) that totally covered the P0-2 peptide sequence were synthesized and used for absorption. On the western blot, the peptide P0-2-4 clearly absorbed the immunoreactivity from the patient serum (Fig. 4C), indicating that the 36-kDa protein has the extra sequence derived from the 3'UTR of P0 mRNA, and the epitope recognized by the serum is located within the P0-2-4 sequence (SRTSLKNALKNM). Thus, because the 36-kDa protein is encoded by the P0 gene, we designated this protein as a large form of myelin P0 and called it L-MPZ. A rabbit polyclonal anti–L-MPZ was produced against a 20-aa peptide (Fig. 4A; anti–L-MPZ antigen peptide) that includes the P0-2-4 sequence. This rabbit anti–L-MPZ antibody recognized the same 36-kDa band as the band detected by the patient serum (Fig. 4D). The high antigenicity of this specific region of L-MPZ was demonstrated by the extremely high titer of this antibody in an ELISA with the peptide antigen (>1/512,000; ~2.0 ng/ml) and western blotting with the ScN homogenate (>1/40,000; ~0.05 μg/ml). The immunoreactivity of anti–L-MPZ was also absorbed by both the antigen peptide and the P0-2-4 peptide (data not shown), which indicates that the epitope for the rabbit antibody and the patient IgG were in the same 12-aa region.

Production of both L-MPZ and P0 from human P0 cDNA–The P0 gene is relatively small (7 kb) and consists of six exons (1). Exon 6 contains both stop codons (Fig. 3A). Therefore, we considered it unlikely that L-MPZ is translated from a splice variant. To test whether L-MPZ was produced from P0 mRNA, we analyzed NIH/3T3 cells transfected with a P0 expression vector containing full-length human P0 cDNA. After electroporation, the human P0 protein was transiently expressed in the NIH/3T3 cells (Fig. 5A). Both glycosylated and deglycosylated (by PNGase F) L-MPZ bands were detected in lysates from transfected NIH/3T3 cells with western blotting using anti–L-MPZ (Fig. 5B).

Aminoglycosides such as G418 are reported to induce stop codon readthrough in *Escherichia coli*, yeast, and human cultured cells (23, 24). To confirm the stop codon readthrough of P0 mRNA, we performed *in vitro* transcription/translation in the presence of G418 using a mammalian *in vitro* transcription/translation system. For effective stop codon readthrough in *in vitro* translation, 5 μg/ml G418 is sufficient (25). Synthesized [^{35}S] methionine-labeled proteins were detected by autoradiography of SDS-PAGE gel (Fig. 6A). Strong band of unglycosylated P0 with the leading peptide (predicted MW: ~27.5 kDa) was detected in the sample from the *in vitro* transcription/translation of human P0 cDNA without G418. Unglycosylated L-MPZ with the leading peptide (predicted MW: ~34.4 kDa) was also detected at low levels in the fraction not treated with G418. A dramatic increase of L-MPZ was detected in the sample with human P0 cDNA in the presence of G418. The relative ratio of P0 and L-MPZ were calculated from the intensity of each band with or without G418 treatment (without G418, P0 107.3±2.8, L-MPZ 16.3±3.3; with G418, P0 57.1±2.2, L-MPZ 81.1±4.9) (%) (Fig. 6B). Next, to demonstrate P0 stop codon readthrough producing L-MPZ, three types of readthrough model mutants as L-MPZ, deletion or replacement (Ala or Tyr) of P0 stop codon in hP0/pcDNA3, were used in *in vitro* translation. All three types of vectors produced the bands corresponding to unglycosylated L-MPZ with the leading peptide (Fig. 6A). These results indicate that both P0 and L-MPZ were derived from P0 mRNA, possibly via stop codon readthrough. Thus, L-MPZ is probably produced in P0-expressing Schwann cells *in vivo* by the same mechanism.

Molecular structure of L-MPZ–The predicted structure of L-MPZ, based on data from western blotting, MS analysis, and the transfection study, is depicted in Figure 7. According to the results from the deglycosylation assay and MS analysis, most of the structure of L-MPZ seems to be identical to that of P0; the N-terminal extracellular region contains a disulfide bond, an Ig-like domain, and N-linked glycosylation. There is a transmembrane region and a C-terminal cytoplasmic region that contains a putative PKC-dependent phosphorylation site. We found that L-MPZ has an extra 63 aa at the C terminus of P0, which are located in the cytoplasm. This additional region is highly basic and may contain an extra PKC-dependent phosphorylation site, which is in the antigenic site. No other known

motifs or domains were found in the L-MPZ–specific extra region.

Developmental expression and localization of L-MPZ in the PNS–L-MPZ was enriched in the adult ScN myelin fraction and was translated from P0 mRNA. Because the expression of P0 protein is dramatically increased during early postnatal development, we next investigated the change in L-MPZ expression by stop codon readthrough during ScN development. L-MPZ and PNS myelin proteins (P0 and MBP-splice variants) were detected with western blotting. In myelin fractions obtained during the various developmental stages, L-MPZ was detected from P1, and expression increased with age, similar to the major PNS myelin proteins (Fig. 8A). Because myelinogenesis is active around P7 in the rat PNS, upregulation of L-MPZ in 5- to 7-day-old rat ScN myelin may be involved in the maturation of myelinated fibers.

To investigate the localization of L-MPZ in the PNS, double immunostaining of adult rat longitudinal ScN sections was performed using anti–L-MPZ (green) and anti-NF (red; Fig. 8B) antibodies. L-MPZ–positive signals were detected specifically in the myelin, which ensheathed NF-positive axons. Thus, L-MPZ is localized in the compact myelin of the PNS.

Cellular localization of L-MPZ and P0 in transfected HeLa cells–During myelination, P0 is targeted to the plasma membrane, and homophilic binding of extracellular Ig-like domains mediates intermembrane adhesion to form compact myelin (2). In the HeLa cell culture system, forcibly expressed P0 protein is localized to the plasma membrane, especially at sites of close apposition between two P0-expressing cells (26). To investigate the cellular localization of L-MPZ and P0, we performed double immunostaining of full-length P0 cDNA–transfected HeLa cells using anti–L-MPZ and anti-P0 antibodies. L-MPZ and P0 immunoreactivities were colocalized (Fig. 9A, first row,). While anti-L-MPZ can detect only L-MPZ, anti-P0 antibody detects mainly P0 but also slightly detects L-MPZ in western blot (Fig. 2A). Therefore, to confirm the individual distribution of P0 and L-MPZ in transfected cells, five types of mutant [deletion or frame-shift mutants to express only P0, deletion or replacement (Ala or Tyr) of P0 stop codon to express only L-MPZ-like molecules] were generated from full-length human P0 cDNA (Fig. 9B). The productions of these mutant molecules were confirmed by western blotting using anti-P0 or anti-L-MPZ antibodies (data not shown). In immunocytofluorescence, both individual P0 and L-MPZ-like molecules were detected in plasma membrane (Fig. 9A, second-6th rows). Especially, just like P0, L-MPZ-positive signals were accumulated at sites of cell-cell adhesion between two L-MPZ-like mutant-expressing cells (Fig. 9A, 4th-6th rows). These results indicate that L-MPZ may also contribute to cell adhesion.

DISCUSSION

In this study, we show that the highly antigenic 36-kDa neuropathy-associated protein, designated L-MPZ, is a novel isoform of P0 that contains an additional 63 aa at the C terminus of P0. This protein is probably produced by translational readthrough of the regular P0 stop codon, because L-MPZ was produced by the identical P0 mRNA in conjunction with P0 in transfected mammalian cells and because P0 peptides and peptides with the deduced aa sequence in the 3′UTR of P0 are both found with MS analysis of tryptic L-MPZ fragments. Stop codon readthrough was also shown by the great increase in L-MPZ synthesis with mammalian *in vitro* transcription/translation system in the presence of G418. P0 stop codon readthrough model mutants those only produced L-MPZ-like proteins were also synthesized by mammalian *in vitro* transcription/translation system. Like P0, L-MPZ was expressed during myelinogenesis, localized in compact myelin of the PNS, and accumulated at cell-cell adhesion sites in transfected cells, suggesting that L-MPZ is involved in the formation and/or maintenance of compact myelin, similar to P0. Because the L-MPZ–specific region contains an additional putative PKC phosphorylation site and is highly antigenic, L-MPZ may also have some unique roles in normal and pathological myelin conditions.

There was a high degree of homology at the aa level among the L-MPZ–specific coding regions in P0 mRNA from mammals and *X. laevis* (>80% identity in mammals and ~48% identity in *X. laevis*), but such homologies were not seen in zebrafish or shark P0 mRNA (data not shown). These findings suggest that evolutionarily, P0 may have acquired the L-MPZ–specific region by stop